Validation and Optimization of Breeding Strategy for miR-141/200c Knockout Mice to Eliminate Off-Target Gene Silencing using FLPo Deleter

Rashmi Srivastava[1#], Sanjeev Kumar Yadav[1#], Mary-Catherine Cormier[1], Katie Lowther[2], Siu-Pok Yee[2], and Rajkumar Verma[1*]

[1]Department of Neurosciences, UConn Health Farmington CT 06030

[2]Center for Mouse Genome Modification, UConn Health, Farmington CT 06030

[#]equal contribution

*Corresponding author

Rajkumar Verma

Assistant professor

Email: raverma@uchc.edu

ABSTRACT

MicroRNAs (miRNAs) of the miR-200 family specifically miR-141 and miR-200c regulate neurogenesis, differentiation, and epithelial–mesenchymal transitions in development and several diseases including cancer and stroke. The STOCK Mirc13^{tm1Mtm} /Mmjax mouse line, which targets the miR-141/200c cluster, was originally generated and described by Park et al. 2012 as a conditional “knockout-first” allele requiring a two-step breeding strategy: FLP recombination to excise lacZ/neo cassettes followed by Cre recombination to delete the floxed miRNA cluster (1). However, subsequent studies either bypassed this step and reported knockouts based on direct crosses with Cre mouse lines, leaving residual lacZ/neo sequences that may silence upstream elements or introduce transcriptional artifacts or rare studies used less efficient FLPe Deleter mice. Here, we present a detailed and refined strategy to conditional miR-141/200c knockouts mice using FLPo Deleter mice to efficiently eliminate lacZ/neo cassettes. Our approach not only confirmed complete deletion of miR-141 and miR-200c in various organs such olfactory bulbs and lungs where these miRNAs are robustly expressed using various approach

such as genotyping qPCR validation and in situ hybridization but showed that without the use of FLPo deleter mice deletion of miR-141/200c cluster amy also lead to loss of several close proximity physiologically important genes such as *ptpn6, phb2, atn1 and eno1 .* By restoring a clean floxed allele using FLPo deleter mice prior to Cre deletion, we establish a reliable and interpretable mouse model for dissecting the roles of the miR-141/200c cluster miRNA in various disease models.

INTRODUCTION

microRNAs (miRNAs) are small, noncoding RNAs (~22 nucleotides) that regulate gene expression post-transcriptionally and play pivotal roles in development and disease. Originally discovered in C. elegans (2,3) and later shown to be evolutionarily conserved across species (4) miRNAs are now recognized as critical regulators in cardiovascular (5,6) neurological (7, 8), and oncogenic pathways (9, 10), holding significant potential for therapeutic applications (7,11) While cell-based studies have elucidated many of these mechanisms, in vivo models with the help of conditional deletion of these miRNAs remain essential to fully understand their functions under physiological and pathological contexts.

Park et al. (1) established a key genetic resource for such investigations by generating conditional knockout-first mouse lines for conserved miRNAs, including the miR-141/200c cluster (Mirc13tm1Mtm/Mmjax). This cluster, located on mouse chromosome 6, encodes two members of the miR-200 family implicated in neurogenesis (12, 13), differentiation (14), epithelial–mesenchymal transition (15) cancer (8,16,17) stroke (6, 18) and Alzheimer's disease (19). In order to make miR-141/200c cluster KO mice, the authors Park et al., used a targeting vector to incorporate lacZ reporter and β-actin-neo selection cassette flanked by FRT sites, and loxP sites surrounding the miR-141/200c cluster, to enable a two-step recombination strategy: first, FLP-mediated removal of the lacZ/neo cassette to generate a clean conditional (floxed) allele, followed by Cre-mediated excision of the cluster (11). However, many subsequent studies bypassed this essential FLP recombination step (20-25) or used inefficient FLPe deleter strains with incomplete recombination (26-28). While the earlier approaches retained the lacZ/neo cassette, which can transcriptionally silence neighboring genes (29, 30) or alter expression patterns due to strong β-actin promoter activity (31), confounding phenotypic interpretation. Recent reports highlight that residual cassettes may inadvertently suppress several close proximity genes e,g Ptpn6, Phb2, Atn1 Eno2 and Eng1 in case of

miR-141/200c cluster, which may play a critical regulatory role of neuronal function and mitochondrial integrity—leading to misleading outcomes or loss of phenotype in the KO mice generated without prior neo cassette deletion.

To overcome these limitations, we optimized the original “knockout-first” design suggested by Park et al. 2012 (1) by employing high-efficiency FLPo deleter mice instead of FLPe or β-actin-FLP strains (32-34). FLPo recombinase exhibits greater thermostability and recombination efficiency in mammalian cells (32-34) ensuring complete excision of the lacZ/neo cassette and restoration of an unperturbed floxed allele before Cre-mediated deletion. This refinement minimizes off-target silencing, preserves adjacent gene expression, and produces genetically clean global or tissue-specific miR-141/200c knockouts. Here, we present a validated, optimized and detailed breeding strategy using FLPo deleter mice that ensures complete removal of the lacZ/neo cassette and precise deletion of the miR-141/200c cluster. This work establishes a robust framework for generating unambiguous cell specific or conditional knockouts of the miR-141/200c cluster, facilitating accurate studies of miRNA function in neural and systemic disease models.

METHODS

Experimental Mice

All mouse strains were obtained from the Jackson Laboratory (Farmington, CT). The STOCK Mirc13^{tm1Mtm}/Mmjax line (RRID: MMRRC_034657-JAX) carries a targeted allele containing a lacZ reporter, β-actin-neo cassette, and floxed miR-141/200c cluster (lacZ-neo-flox). These are referred to as miR-141/200c knockout (KO) mice throughout this study. The B6.129S4-Gt(ROSA)26Sor^{tFLP})Sor/J (ROSA-FLPo) strain (RRID: IMSR_JAX:012930) expresses a highly efficient FLPo recombinase driven by the CAG promoter. Additional Cre-driver lines included Hprt-Cre (129S1/Sv-Hprt1^{tm1(CAG-cre)Mnn}/J; RRID: IMSR_JAX:004302) and LysM-Cre (B6.129P2-Lyz2^{tm1(cre)Ifo}/J; RRID: IMSR_JAX:004781). Female Hprt-Cre mice express Cre recombinase under the PGK promoter, enabling early deletion of loxP-flanked sequences during zygotic or early cleavage stages.

All mice were maintained under standard conditions (ambient temperature and humidity) with ad libitum access to pellet food and water.

Genomic DNA Isolation

Tail biopsies (~4 mm) were collected in DNase-free microtubes and digested overnight at 56 °C in 40 µL of lysis buffer (25 mM NaOH, 0.2 mM EDTA) containing 1 µL Proteinase K. Samples were then heated to 100 °C for 1 hour, neutralized with 40 µL Tris buffer (40 mM, pH 7.5), and DNA was precipitated using an equal volume of ice-cold isopropanol. The pellet was washed and resuspended in 30 µL DNase-free water for PCR.

PCR Amplification and Agarose Gel Electrophoresis

Genotyping was performed using primer pairs listed in Table 1. All primers were obtained from the Jackson Laboratory database except for the forward primer for the miR-KO allele (P10), designed in this study to confirm deletion of the miR-141/200c cluster (Fig. 1a, Table 1). PCR reactions (25 µL) contained 2× JumpStart™ Taq ReadyMix (Sigma-Aldrich P2893), 50 ng genomic DNA, and 0.2 µM of each primer. Cycling conditions were: 94 °C for 3 min; 35 cycles of 94 °C for 30 s, primer-specific annealing, 72 °C for 30–45 s; and a final extension at 72 °C for 4 min. PCR products were separated on 2% agarose gels prepared in 1× Tris-Acetate-EDTA (TAE) buffer (Bio-Rad 1610743) with SYBR™ Safe DNA stain (Invitrogen S33102) and visualized under UV illumination.

Global Knockout Line Maintenance

Heterozygous KO/+ mice were intercrossed to generate KO/KO homozygotes for experimental analyses. KO/+ heterozygotes were used to maintain the colony, and wild-type littermates served as age- and sex-matched controls.

Tissue-Specific Knockout Line Maintenance

miR-141/200c^{fl/fl}, LysM-Cre/+ mice were crossed with fl/fl WT mice to generate fl/fl, LysM-Cre/+ (experimental) and fl/fl, WT (control) offspring. To avoid Lyz2 gene disruption, LysM-Cre/LysM-Cre homozygotes were not bred.

β-Galactosidase (lacZ) Staining

A β-galactosidase staining kit (Sigma-Aldrich GALS) was used to assess lacZ reporter expression. Mice were deeply anesthetized with Avertin (250 mg/kg, i.p.), perfused with ice-cold PBS, and brains were collected. Cryosections (10 μm, Superfrost Plus slides) were fixed for 10 min, incubated with X-Gal solution (40 mg/mL) at 37 °C for 0.5–2 h, rinsed in PBS, mounted in 70% glycerol, and imaged under bright-field microscopy.

RNA Isolation, cDNA Synthesis, and Real-Time PCR

Total RNA (including small RNA) was extracted from brain regions (olfactory bulb, frontal and parietal cortex, hippocampus, cerebellum) and peripheral organs (heart, lung, liver) using TRIzol or miRVana kits (Ambion Life Technologies). cDNA synthesis for miRNAs and mRNAs was performed using the TaqMan MicroRNA Reverse Transcription Kit (Thermo Fisher 4366596) and iScript cDNA Synthesis Kit (Bio-Rad 1708891), respectively. TaqMan assays included miR-141-3p (000463), miR-200c-3p (002300), U6 (001973), Ptpn6 (Mm00469153_m1), Phb2 (Mm00476104_m1), Atn1 (Mm00492256_m1), Eno2 (Mm00469062_m1), Emg1 (Mm00496596_m1), and Gapdh (Mm99999915_g1) (Thermo Fisher Scientific). Reactions were run with TaqMan Universal PCR Master Mix II (No UNG; Thermo Fisher 4440040). Relative expression was determined by the 2^–ΔΔCt method using U6 and Gapdh as normalizers for miRNA and mRNA targets, respectively.

RNA Fluorescence In Situ Hybridization (RNA-FISH)

RNA-FISH was performed using Molecular Instruments protocols. Fixed tissue sections were pre-hybridized at 37 °C and incubated overnight with 1.6 pmol of the miR-141-3p probe. Following stringent SSCT washes, signal amplification was performed using snap-cooled hairpins (h1/h2; 6 pmol each) incubated overnight at room temperature. Sections were mounted with antifade DAPI UltraCruz Mounting Solution (Santa Cruz SC-24941) and imaged by fluorescence microscopy.

Statistical Analysis

Data are presented as mean ± SD. Statistical analyses were performed using GraphPad Prism 10.5 (San Diego, CA). Student’s t-test was used for comparisons between two groups, and $p < 0.05$ was considered statistically significant.

Gene targeted	Direction and Name	Primer Sequence (5'-3')	Amplicon size
Targeted miR cluster-generating site	Forward Primer (P5)	CAA CAG CCT CTG ACC TTT AAC C	432bp
	Reverse Primer (P6)	CCT TCT GGG CAG ACA AGA ATA C	
miR cluster-generating site (WT)	Forward Primer (P5)	CAA CAG CCT CTG ACC TTT AAC C	340bp
	Reverse Primer (P6)	CCT TCT GGG CAG ACA AGA ATA C	
lacZ	Forward Primer (P1)	ATC CTC TGC ATG GTC AGG TC	315 bp
	Reverse Primer (P2)	CGT GGC CTG ATT CAT TCC	
β-actin-neo cassette	Forward Primer (P3)	CTT GGG TGG AGA GGC TAT TC	280bp
	Reverse Primer (P4)	AGG TGA GAT GAC AGG AGA TC	
mir KO (mir5'Fn3')	Forward Primer (P10)	CCG GCA GGT GAA GGA GGA AG'	~300 bp
	Reverse Primer (P6)	CCT TCT GGG CAG ACA AGA ATA C	
FLPo	Forward Primer (P7)	AAA GTC GCT CTG AGT TGT TAT	300 bp
	Reverse Primer (P8)	GCG AAG AGT TTG TCC TCA ACC	
	Forward Primer (P7)	AAA GTC GCT CTG AGT TGT TAT	603 bp
	Reverse Primer (P9)	GGA GCG GGA GAA ATG GAT ATG	

HprtCre (Cre recombinase)	Forward Primer (P11)	GCG GTC TGG CAG TAA AAA CTA TC	100 bp
	Reverse Primer (P12)	GTC AAA CAG CAT TGC TGT CAC TT	
LysMCre (Cre recombinase)	Forward Primer (P13)	CTT GGG CTG CCA GAA TTT CTC	700bp
	Reverse Primer (P14)	CCC AGA AAT GCC AGA TTA CG	
	Forward Primer (P13)	CTT GGG CTG CCA GAA TTT CTC	350 bp
	Reverse Primer (P15)	TTA CAG TCG GCC AGG CTG AC	

Table1. List of different sets of primer sequences (with amplicon size) used in PCR amplification

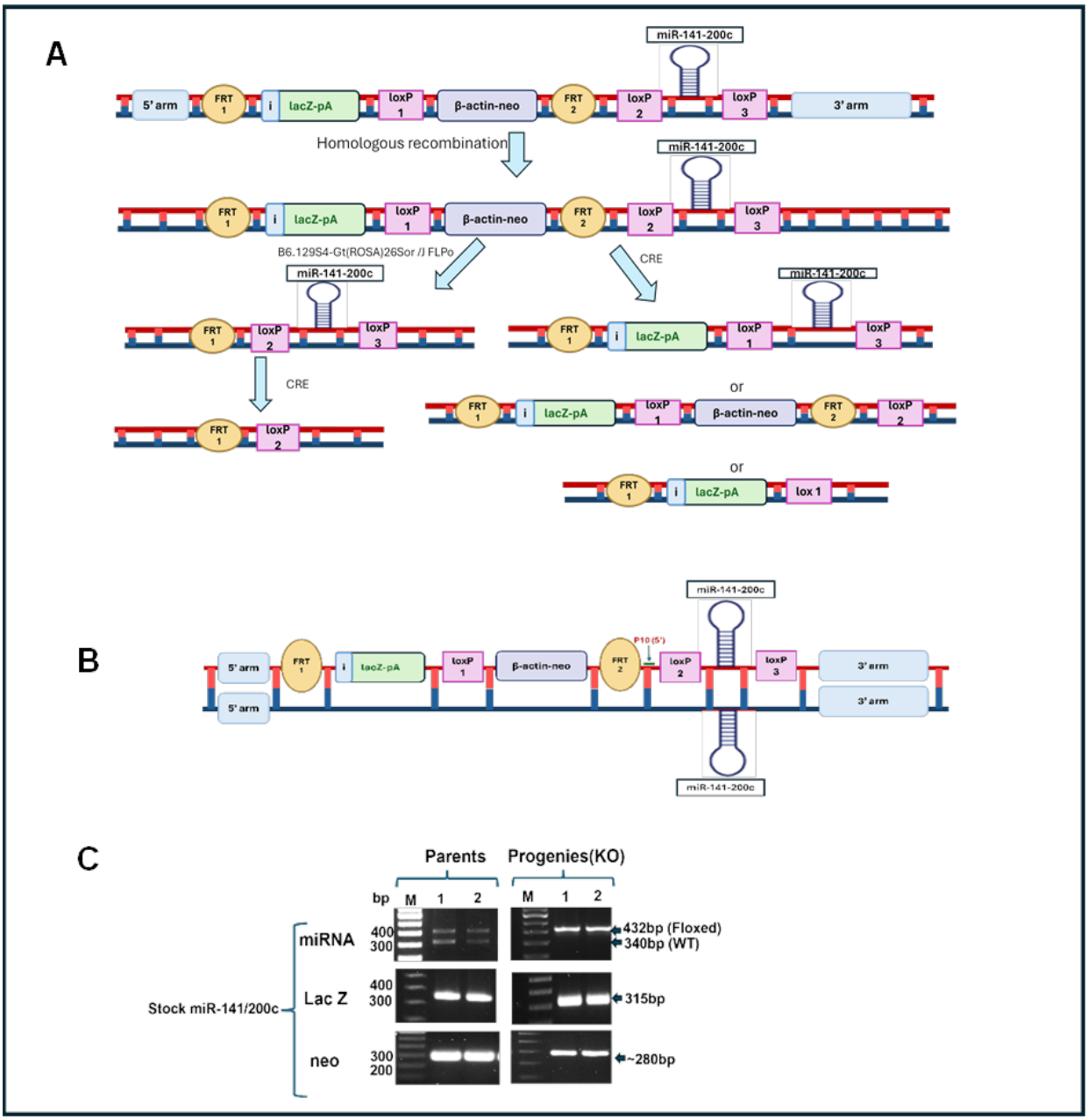

Figure 1: a) *Schematic representation of the gene targeting strategy and allele modification process for conditional knockout generation. The top panel ("Targeting Vector") illustrates the original targeting construct containing 5' and 3' homologous arms, a lacZ reporter with polyadenylation signal (lacZ-pA), loxP and FRT sites, and a β-actin-neo selection cassette. The middle panel ("Targeted Allele") shows the correctly integrated targeted allele after homologous recombination, with all key elements positioned between loxP and FRT sites. The lower panels illustrate recombinase-mediated excision outcomes: FLP recombinase excises the β-actin-neo cassette at FRT sites, and Cre recombinase mediates excision at different combinations of loxP sites*

(loxP1/loxP2, loxP2/loxP3, or loxP1/loxP3), yielding multiple possible allelic configurations. These steps enable precise control over gene disruption and regulatory element removal, facilitating conditional knockout and downstream genetic analyses. ***b)*** *Representation of Primer position binding on the targeted allele: Forward primer (P10) was designed to screen homozygous miR-141/200c-knockout (miR-KO) so that it binds to the upstream of loxP-2 site which is also upstream of mir-141/200c allele.* ***c)*** *PCR validation of miR-141-200c alleles and the generation of homozygous knockout of miR-141/200c: Agarose gels showing PCR-genotyping results of targeted alleles in parents (first set) and screening of progenies on 2% agarose gels (second set) where miRNA (miR-141/200c), lacZ, neo are showing the PCR results of their expression. Lane M is the DNA ladder lane, lanes-1 and 2 are mouse #1 and mouse#2. PCR analysis of genomic DNA from various mouse lines shows expected band sizes corresponding to wild-type (WT) and mutant (Mut) alleles for both miR-141-200c floxed and FLPo gene constructs. Bands at 280 bp, 300 bp, 315 bp, and 340 bp confirm genotype status across samples.*

RESULTS

Breeding Strategies for the Generation of miR-141/200c Knockout Mice

To compare the outcomes of miR-141/200c deletion by either direct crossing the MirC13 colony or with prior deletion of neo cassette by FLPo deleter mice, we present following two detailed breeding schemes

Strategy 1 (S1): Generation of Homozygous Knockout Mice from Stock miR-141/200c Lines

Cross: Stock miR-141/200c $^{+/-}$ × Stock miR-141/200c$^{+/-}$

The STOCK miR-141/200c line was originally designed as a conditional lacZ-reporter-tagged knockout-first strain for the miR-141/200c cluster (1). The strong polyadenylation signal within the β-actin–neo cassette terminates transcription, effectively silencing downstream miR-141/200c expression. Prior to breeding, stock mice received from Jackson were PCR-genotyped to confirm the presence of the lacZ–neo–flox allele (Fig. 1c). Homozygous knockouts (S1GKO) were generated by intercrossing validated heterozygotes ($^{+/-}$) and offspring were genotyped by PCR for the wild-type (WT, $^{+/+}$),

heterozygous ($^{+/-}$) and homozygous ($^{-/-}$)alleles. Amplicons for the miR-141/200c locus yielded 340 bp (WT) and 432 bp (KO) products, whereas heterozygotes showed both bands. Amplicons corresponding to lacZ and β-actin–neo alleles appeared at 315 bp and 280 bp, respectively, in heterozygous and homozygous offspring (Fig. 1c). These results confirmed successful homologous recombination and insertion of the lacZ–neo–flox cassette, establishing the S1GKO line for subsequent validation and phenotypic studies.

Strategy 2 (S2): Two-Step Generation of Global and Conditional Knockouts Using FLPo and Cre Recombinases

Step 1: FLPo-Mediated Excision of the lacZ/neo Cassette

***Cross:* Stock miR-141/200c × ROSA-FLPo**

To remove the reporter and lacZ/neo cassette, stock miR-141/200c $^{(+/-)}$ mice were crossed with ROSA-FLPo mice (RRID: IMSR_JAX:012930). Offspring were PCR-genotyped to detect excision of the lacZ–neo cassette and inheritance of the FLPo allele. PCR analysis revealed complete excision in pups #1 and #2, while residual lacZ amplicons (315 bp) persisted in pups #3, reflecting incomplete recombination at the FRT sites (Fig. 3a).

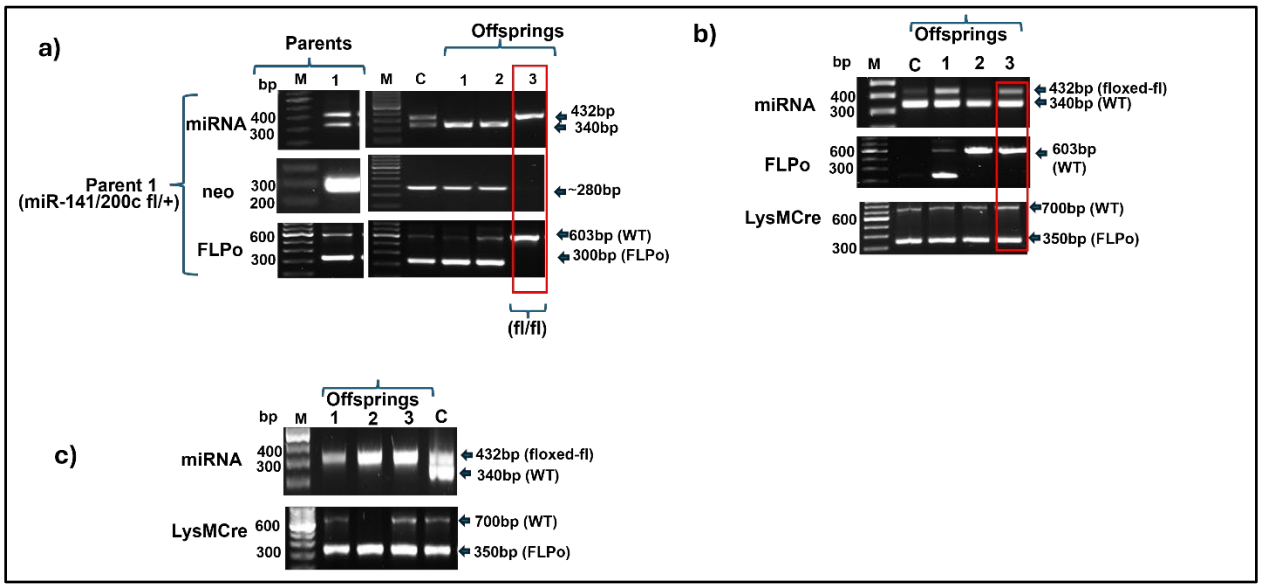

Fig.2 Generation of myeloid cell-specific homologous knockout of miR-141/200c. Multiple PCR panels indicate confirmation of floxed miR clusters, generic neo, FLPo, and LysMCre in various breeding strategies. Reproducible gel bands evidence the presence of all intended elements in offspring after the crosses. Agarose gel electrophoresis: ***a****) presents PCR genotyping for miR141-200c fl/+, FLPo/+ × miR141-200c fl/+, FLPo/+*

progeny, verifying the presence of floxed miR cluster, generic neo, and FLPo alleles, ***b****) depicts results of miR141-200c fl/+, FLPo/+ × LysMCre/+ crosses, confirming the successful integration of the LysMCre transgene and one of the floxed alleles in the selected mice.* ***c****) confirms the integration of LysMCre and presence of floxed alleles on both the loci. Banding patterns and schematics detail the genotype structure in each experimental line. Lane M is the DNA ladder lane, lane C is the positive controls of the respective PCR, lanes-1, 2 and 3 are respective mouse #1, #2 and #3.*

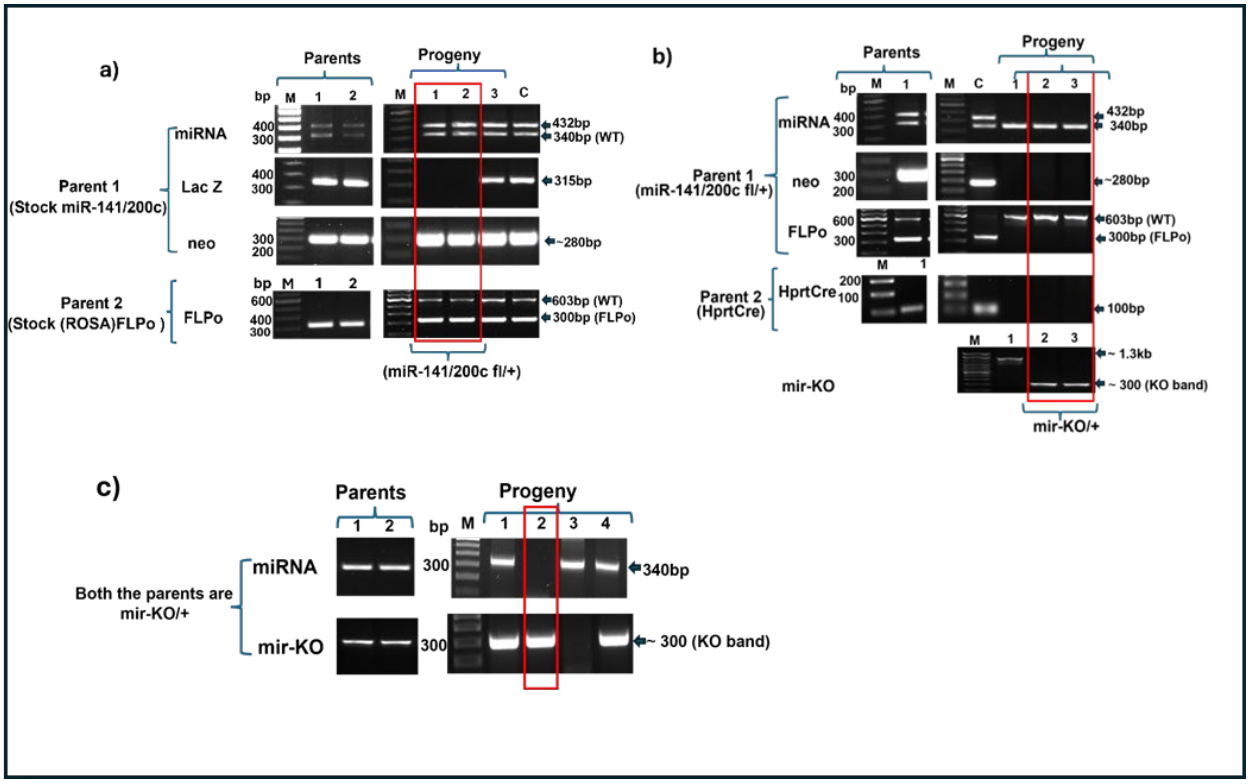

Figure. 3. Genotype screening of transgenic mice. *Agarose gels showing PCR results of targeted alleles in parents (first set) and progeny screening on 2% gels (second set).* ***a****) Generation of heterozygous conditional knockouts mediated by FLP alleles. Offspring yielding a 603 bp FLPo amplicon, 432bp (floxed miR-141/200c) and loss of the lacZ allele were selected for further breeding with Cre deleter mice.* ***b****) Generation heterozygous miR-141/200c knockout (mir-KO/+) mediated by Cre. Offspring from the crossing of floxed miR-141/200c with HprtCre mice were PCR-genotyped for the targeted allele (miRNA), neo, FLPo and HprtCre. The homozygous miR-141/200c knockout mice were selected which showed WT for miR-141/200c (340bp), FLPo (603bp), neo (no band) and HprtCre*

(no band) genotype, and loss of floxed-mir-141/200c allele (~300bp). ***c****) Generation of litter- and aged- offsprings from crossing mir-KO/+ male mice with HprtCre female mice. PCR-genotyping of offsprings for the miR-141/200c showed either WT band and KO band.*

This breeding step yielded heterozygous miR-141/200c (fl/+) FLPo/+ conditional knockout (CKO) alleles suitable for further crosses. We can use these mice for generation of either homozygous miR141/200c (fl/fl) for cell specific mice generation by crossing it with cell specific Cre or to generate global miR 141/200c (-/-) mice by directly crossing with Hprt cre

Step 2: Generation of homozygous (fl/fl) mice for conditional KO mice generation

Cross: miR-141/200c (fl/+) FLPo/+ × miR-141/200c (fl/+) , FLPo/+

We generated miR-141/200c$^{(fl/fl)}$ CKO mice by inter-crossing miR-141/200c (fl/+), FLPo/+ mice. Progeny that was homozygous for the miR floxed CKO allele (432bp) and WT (603bp) for the (ROSA)FLPo were selected (Fig.3a) to bred out the FLPo gene. Once homozygous floxed (CKO) mice have been established, breeding to produce tissue-specific knockouts—such as myeloid-specific deletions—becomes significantly more efficient, since every cross with a Cre-driver yields the desired flox/flox;Cre genotype[23].

Step 2a: Myeloid-Specific Deletion via LysM-Cre

Cross: miR-141/200c (fl/+) FLPo/+ × LysM-Cre$^{+/-}$

Heterozygous LysM-Cre mouse were crossed with miR-141/200c (fl/+) FLPo$^{+/-}$ to produce tissue-specific miR-141/200c knockout offspring (miR-141/200c$^{fl/+}$, LysM-Cre$^{+/-}$). Pup #3 inherited both the floxed miR (fl/fl) allele and LysM-Cre transgene and was selected as tissue-specific miR-141/200c heterozygous where FLPo and associated neo sequences were bred out in this generation (Fig. 3b).Step 2b: Generation of tissue-specific miR-141/200c$^{-/-}$ miceCross: miR-141/200c$^{fl/+}$, LysM-Cre$^{+/-}$ x miR-141/200c$^{fl/fl}$

Breeding of miR-141/200c$^{fl/+}$, LysM-Cre$^{+/-}$ mouse with miR-141/200c$^{fl/fl}$ mouse yielded pups those are miR-141/200c$^{fl/fl}$, LysM-Cre$^{+/-}$ and miR-141/200c$^{fl/fl}$, LysM-Cre$^{-/-}$

littermates. Pups # 1 and #3 showed miR-141/200c$^{fl/fl}$, LysM-Cre$^{+/-}$ genotype whereas pup#2 had miR-141/200c$^{fl/fl}$, LysM-Cre$^{-/-}$ genotype (Fig. 3c).

Step 2b: FLPo-Cleaned Global Knockout via Cre-Mediated Excision

Cross: miR-141/200c ($^{fl/+)}$FLPo$^{+/-}$ × Hprt-Cre$^{+/-}$

As we discussed earlier, we can generate miR-141/200c$^{-/-}$ mice by crossing miR-141/200c$^{(fl/fl)}$ CKO male mice with female Hprt-Cre$^{+/-}$ mice. We achieved alternate strategy to generate littermate global miR-141/200c$^{-/-}$ and WT mice by crossing miR-141/200c ($^{fl/+)}$FLPo$^{+/-}$ male mouse with Hprt-Cre$^{+/-}$ female mouse. Progenies which were inheriting floxed allele (fl/+) and Hprt-Cre transgene displayed recombination at the two remaining loxP sites, resulting in excision of the miR-141/200c cluster and generation of a global knockout allele (Fig. 3b & c).

PCR genotyping confirmed successful deletion: WT alleles produced a 340 bp band, while miR-141/200c-KO alleles yielded a 300 bp amplicon. Offspring such as pups #2 and #3 showed the heterozygous miR-141/200c-KO (miR 141/200c $^{-/+}$) genotype, indicating efficient recombination. Because the Hprt-Cre transgene is X-linked and expressed during oogenesis, recombination occurred before fertilization, enabling excision at the one- or two-cell stage. Importantly, selected heterozygous mice had the Hprt-Cre and FLPo alleles bred out, producing clean heterozygous knockouts (miR$^{-/+}$) for line establishment (Fig. 3b).

Cross: miR-141/200c $^{(+/-/+)}$× miR-141/200c $^{(+/-)}$

miR-141/200c$^{(+/-)}$ mice were intercrossed to generate littermate global miR-141/200c$^{-/-}$ and WT mice (Fig. 3c)

***Expression Analysis of miR-141-3p and miR-200c-3p in mice from* strategy 1 (S1GKO)**

Expression of miR-141-3p and miR-200c-3p was initially assessed using lacZ reporter staining. Strong lacZ activity was detected in the olfactory bulb, with weaker staining near the lung–tracheal junction, and minimal expression in heart or liver (Fig. 4A). RT-qPCR confirmed high basal expression of both miRNAs in the olfactory bulb and lung of WT

mice (ΔCt < 5), consistent with the miRNA expression atlas (35) ((Fig. 4B–C). In S1GKO mice, RT-qPCR revealed near-complete loss of both miRNAs in the olfactory bulb and a substantial reduction in the lungs (Fig. 4D–G).

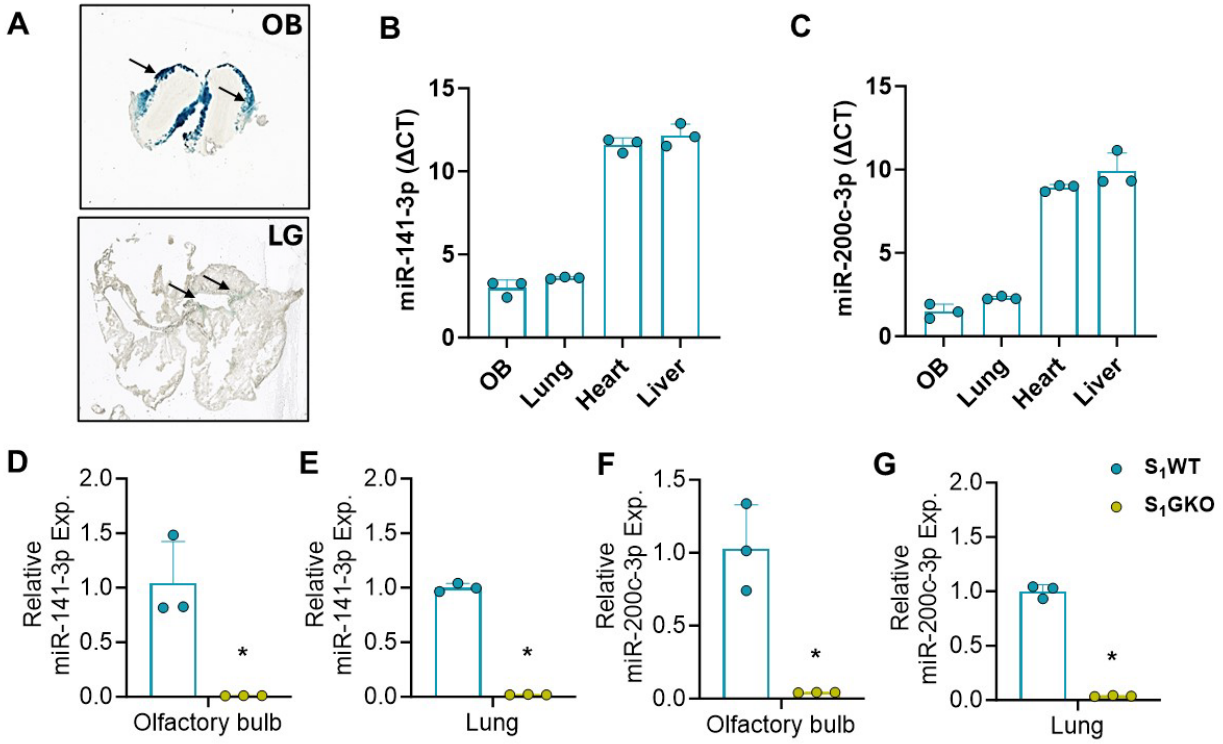

Fig 4. Expression analysis of miRNA-141/200c. miRNA-141/200c expression analyzed by lacZ reporter expression and RT-qPCR in 6–8-week-old mice. Olfactory bulb (OB) exhibited strong lacZ reporter expression for miR-141/200c whereas the lung (LG) showed localized staining near the respiratory tract attachment site (A). The basal expression of miR-141-3p and miR-200c-3p was analyzed by RT-qPCR in the brain olfactory bulb and other peripheral organs such as the lung, heart, and liver of wild-type mice. The data showed that miR-141-3p and miR-200c-3p were highly expressed in the olfactory bulb and lung (ΔCT < 5), whereas heart and liver exhibited lower expression levels (ΔCT > 10) (B&C). Total RNA was isolated from the brain olfactory bulb and lungs of wild-type and lacZ KO mice generated by strategy one (S_1), and relative expressions of miR-141-3p and miR-200c-3p were assessed by RT-qPCR. A significant and near-complete reduction of miR-141-3p and miR-200c-3p expression was observed in the olfactory bulb and lungs (D-G). Data are presented as mean ± SD (*$p < 0.05$ vs. WT control).

Expression Analysis of miR-141-3p and miR-200c-3p in mice from **Strategy 2 (S2GKO)**

Using the optimized FLPo-first, Cre-second approach, global KO mice (S2GKO) and matched WT controls (S2WT) were generated. In S2WT mice, miR-141-3p and miR-200c-3p showed highest expression in the olfactory bulb and minimal levels in other brain regions (ΔCt > 10) (Fig. 5A–B). In contrast, S2GKO mice exhibited near-complete ablation of both miRNAs across all brain regions, most prominently in the olfactory bulb, as confirmed by RT-qPCR and RNA-FISH (Fig. 5C–M).

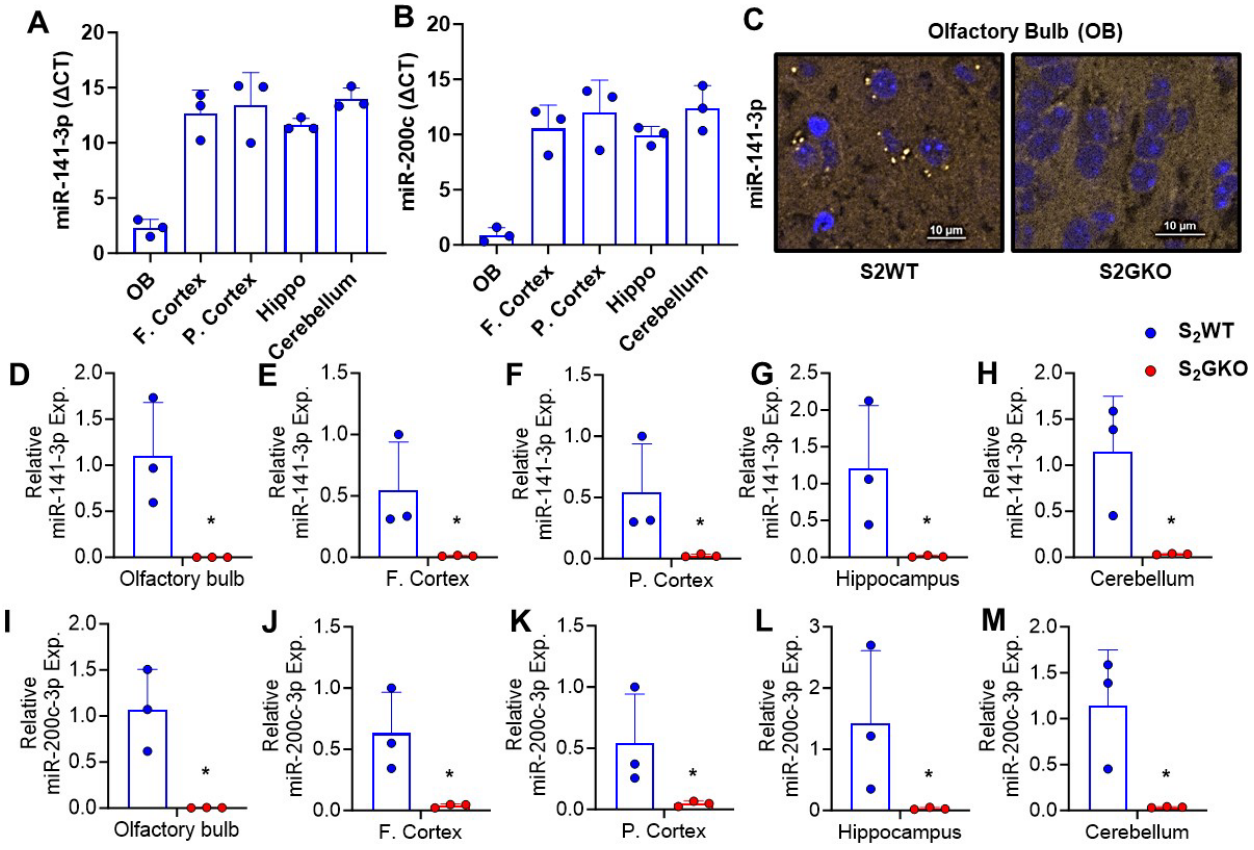

Fig.5 Expression analysis of miR-141-3p and miR-200c-3p in mice generated by strategy 2. Total RNA was isolated from the olfactory bulb (OB), frontal cortex (FC), parietal cortex (PC), hippocampus (HP), and cerebellum (CB) of wild-type (S2WT) and knockout (S2GKO) mice. Basal expression levels of miR-141-3p and miR-200c-3p were assessed

by RT-qPCR in S2WT samples. Both miR-141-3p and miR-200c-3p were highly expressed in the OB ($\Delta CT < 5$), while their expression in other regions was very low ($\Delta CT > 10$) (A&B). Notably, the OB of S2GKO mice showed no detectable expression of miR-141-3p by RNA-FISH (C). This finding was further confirmed by RT-qPCR, which demonstrated a marked reduction of both miRNAs (miR-141-3p & miR-200c-3p) in the OB almost negligible (D&I), along with significantly decreased expression in the FC, PC, HP, and CB of S2GKO mice (E-H & J-M). Data are presented as mean ± SD (*$p < 0.05$ vs. WT control).

Effect of Deletion Strategy on Neighboring Gene Expression

Efficient removal of the lacZ/neo cassette by FLPo recombinase is critical to avoid unintended transcriptional interference with neighboring genes. Retention of this cassette, as in Strategy 1, can alter expression of adjacent loci. To test this, expression of nearby genes (Ptpn6, Phb2, Atn1, Eno2, and Emg1) was analyzed in olfactory bulb tissue by RT-qPCR. In S1GKO mice, Ptpn6, Phb2, and Atn1 were significantly downregulated (>7-fold, >3-fold, and >1.5-fold respectively; $p < 0.05$) compared with WT (Fig. 6A–C). Eno2 and Emg1 also trended downward, though not significantly (Fig. 6D–E). In contrast, S2GKO mice showed no significant changes in any of these genes relative to WT (Fig. 6F–J). These results demonstrate that retention of the lacZ/neo cassette in S1 knockouts can disrupt transcription of nearby genes, whereas the FLPo-first S2 strategy produces genetically clean knockouts, preserving the expression of adjacent elements.

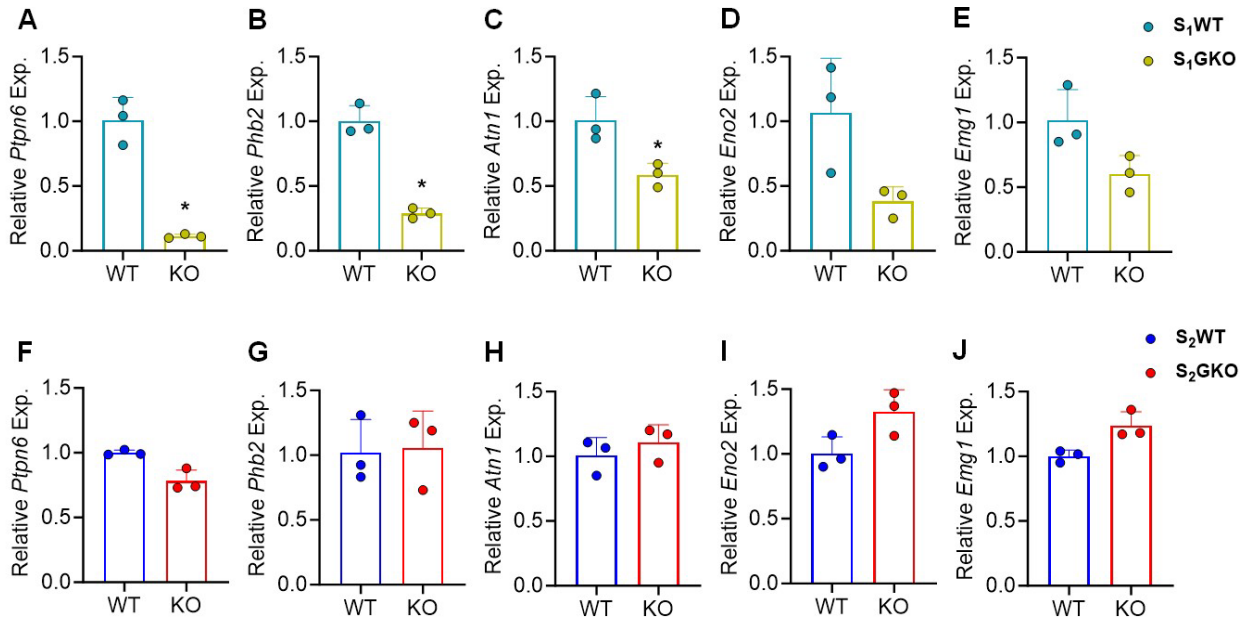

Fig. 6 Expression analysis of neighboring genes in mice generated by strategy 1 and strategy 2. Total RNA was isolated from the olfactory bulb (OB) of knockout (S1GKO and S2GKO) and littermate wild-type (S1WT and S2WT) mice. Expression of Ptpn6, Phb2, Atn1, Eno2, and Emg1 were assessed by RT-qPCR in knockout samples. In strategy 1 knockout (S1GKO) mice, the expression Ptpn6, Phb2, and Atn1 was significantly decreased (±>1.5 folds threshold, $p<0.05$) compared to wild type (S1WT) (A-D), while Eno2 and Emg1 showed a similar decreasing trend (D&E). In strategy 2 knockout (S2GKO) mice, the expression Ptpn6, Phb2, Atn1, Eno2, and Emg1 did not show significantly change (±>1.5 folds threshold, $p<0.05$) compared to wild type (S2WT) (F-J). Data are presented as mean ± SD (*$p < 0.05$ vs. WT control).

DISCUSSION

The generation of the *mirc13tm1Mtm/Mmjax* line by Park et al. 2012 (1) provided the first conditional knockout-first model for the miR-141/200c cluster. In their design, the targeting vector introduced a lacZ reporter and β-actin-neo cassette flanked by FRT sites, in addition to loxP sites bracketing the cluster. Park et al. explicitly recommended a two-step strategy: (1) cross with Flp deleter mice to remove the lacZ/neo cassette and restore a clean conditional (floxed) allele; and (2) use Cre recombinase to achieve either tissue-specific or global deletion of the miR-141/200c cluster. This approach avoids interference from the lacZ/neo elements, which can otherwise silence adjacent genes or alter expression patterns (36, 37). With a splice acceptor, the lacZ tag is fused to the upstream

genetic element and spatiotemporally expressed in a manner reflecting the upstream genetic element's expression(38). While useful for expression analysis, this tag may influence the activity of the upstream genetic element to which it is bound(38). Additionally, the poly(A) tail at the end of the lacZ tag terminates transcription, preventing the complete transcription of the element in which it is embedded and silencing any downstream elements (39). The β-actin-neo cassette, comprising the powerful β-actin promotor and neomycin-resistance gene, is expressed regardless of the lacZ tag's presence due to said powerful promotor. Used during mouse line development to differentiate between nonhomologous and homologous recombination of the targeting vector in ES cell colonies, the β-actin-neo cassette can influence transcription of downstream genes in an unpredictable fashion (40). It is for these reasons that both the lacZ tag and the β-actin-neo cassette must be removed prior to experimental use. Our qPCR data further confirm these unwanted deletion on many close proximity genes such as *ptpn6, phb2 and atn1.* The genes like *ptpn6, phb2, and atn1* each play critical roles in brain function. *ptpn6* regulates microglial signaling and helps restrain neuroinflammation; its loss can drive excessive immune activation and neuronal injury (41). *phb2* maintains mitochondrial integrity and neuronal survival, so deletion can impair energy metabolism and cognitive functions (42). *atn1* acts as a transcriptional co-regulator in neuronal development, and disruption can lead to abnormal differentiation, connectivity, or neurodegeneration (43). Thus, downregulation of these genes as shown by strategy 1 could have significant consequences for neuronal health and brain function. While no chang in these gene in strategy 2 suggests importance of later strategy while breeding.

Despite this clear roadmap, several subsequent studies that employed the *mirc13tm1Mtm/Mmjax* mice appear not to have followed Park's recommended strategy. Instead, direct crosses of the lacZ-neo-flox allele to Cre deleter lines were reported as sufficient to generate knockout mice (20-25). While this strategy (strategy 1) produces a lacZ-tagged null allele, it also retains the β-actin-neo cassette, raising the possibility of unintended transcriptional interference and complicating phenotype interpretation as discussed above. Incomplete reporting of breeding schemes, or reliance solely on the absence of lacZ as a surrogate for knockout status has created ambiguity in the literature regarding the true genetic state of these animals(1). Though some researchers had used β-actin-Flpe mice before crossing with Cre deleter lines, but FLPe recombinase has very

low recombination efficiency in cells and in vivo with mosaic recombination found in almost all embryonic stem cell (26-28). We used (Rosa)FLPo which has better recombination efficiency and are broadly expressed than (β-actin) FLPe in mammalian cells (32-34) .Our study addresses this gap by implementing the complete breeding strategy and detailed step wise protocol expended from original study (1). We also provide qPCR confirmation data in addition to lacZ staining and miRNA FISH. We first removed the lacZ/neo cassettes using (ROSA)FLPo mice, generating a clean floxed allele. Only then did we introduce Cre recombinase, either germline (Hprt-Cre) to achieve global deletion or tissue-specific (LysM-Cre) for lineage-restricted ablation. These steps ensure that any observed phenotype can be attributed directly to loss of the miR-141/200c cluster, without confounding contributions from transcriptional silencing or residual neomycin cassette effects.

This refinement is not merely technical but critical for functional interpretation. Studies of the miR-200 family—including their roles in late postnatal neurogenesis (13), stem cell differentiation (14), and cancer biology (15-17) rely heavily on precise gene dosage and context. Misinterpreted allele structures could mask subtle phenotypes or yield spurious results, contributing to discrepancies across reports. By clarifying the breeding approach and providing critical data supporting the success of our mouse model generation, our work provides a framework for generating unambiguous global and conditional knockouts of the miR-141/200c cluster.

Acknowledgment: This work was supported by NIH, United States (1R21NS114981 and R01 NS140176) and REP Convergence (OVPR UConn, United States) grant to R.V.

References:

1. Park CY, Jeker LT, Carver-Moore K, Oh A, Liu HJ, Cameron R, Richards H, Li Z, Adler D, Yoshinaga Y, Martinez M, Nefadov M, Abbas AK, Weiss A, Lanier LL, de Jong PJ, Bluestone JA, Srivastava D, McManus MT. A resource for the conditional ablation of microRNAs in the mouse. Cell Rep. 2012 Apr 19;1(4):385-91. doi: 10.1016/j.celrep.2012.02.008. PMID: 22570807; PMCID: PMC3345170.
2. Lee RC, Feinbaum RL, Ambros V. The C. elegans heterochronic gene lin-4 encodes small RNAs with antisense complementarity to lin-14. Cell. 1993 Dec 3;75(5):843-54. doi: 10.1016/0092-8674(93)90529-y. PMID: 8252621.

3. Wightman B, Ha I, Ruvkun G. Posttranscriptional regulation of the heterochronic gene lin-14 by lin-4 mediates temporal pattern formation in C. elegans. Cell. 1993 Dec 3;75(5):855-62. doi: 10.1016/0092-8674(93)90530-4. PMID: 8252622.
4. Pasquinelli AE, Reinhart BJ, Slack F, Martindale MQ, Kuroda MI, Maller B, Hayward DC, Ball EE, Degnan B, Müller P, Spring J, Srinivasan A, Fishman M, Finnerty J, Corbo J, Levine M, Leahy P, Davidson E, Ruvkun G. Conservation of the sequence and temporal expression of let-7 heterochronic regulatory RNA. Nature. 2000 Nov 2;408(6808):86-9. doi: 10.1038/35040556. PMID: 11081512.
5. van Rooij E, Kauppinen S. Development of microRNA therapeutics is coming of age. EMBO Mol Med. 2014 Jul;6(7):851-64. doi: 10.15252/emmm.201100899. PMID: 24935956; PMCID: PMC4119351.
6. Small EM, Frost RJ, Olson EN. MicroRNAs add a new dimension to cardiovascular disease. Circulation. 2010 Mar 2;121(8):1022-32. doi: 10.1161/CIRCULATIONAHA.109.889048. PMID: 20194875; PMCID: PMC2847432.
7. Verma R, Ritzel RM, Harris NM, Lee J, Kim T, Pandi G, Vemuganti R, McCullough LD. Inhibition of miR-141-3p Ameliorates the Negative Effects of Poststroke Social Isolation in Aged Mice. Stroke. 2018 Jul;49(7):1701-1707. doi: 10.1161/STROKEAHA.118.020627. Epub 2018 Jun 4. PMID: 29866755; PMCID: PMC6019570.
8. Wu Q, Ye X, Xiong Y, Zhu H, Miao J, Zhang W, Wan J. The Protective Role of microRNA-200c in Alzheimer's Disease Pathologies Is Induced by Beta Amyloid-Triggered Endoplasmic Reticulum Stress. Front Mol Neurosci. 2016 Dec 8;9:140. doi: 10.3389/fnmol.2016.00140. PMID: 28008308; PMCID: PMC5143617.
9. Humphries B, Yang C. The microRNA-200 family: small molecules with novel roles in cancer development, progression and therapy. Oncotarget. 2015 Mar 30;6(9):6472-98. doi: 10.18632/oncotarget.3052. PMID: 25762624; PMCID: PMC4466628.
10. Jin T, Suk Kim H, Ki Choi S, Hye Hwang E, Woo J, Suk Ryu H, Kim K, Moon A, Kyung Moon W. microRNA-200c/141 upregulates SerpinB2 to promote breast cancer cell metastasis and reduce patient survival. Oncotarget. 2017 May 16;8(20):32769-32782. doi: 10.18632/oncotarget.15680. PMID: 28427146; PMCID: PMC5464826.

11. Janssen HL, Reesink HW, Lawitz EJ, Zeuzem S, Rodriguez-Torres M, Patel K, van der Meer AJ, Patick AK, Chen A, Zhou Y, Persson R, King BD, Kauppinen S, Levin AA, Hodges MR. Treatment of HCV infection by targeting microRNA. N Engl J Med. 2013 May 2;368(18):1685-94. doi: 10.1056/NEJMoa1209026. Epub 2013 Mar 27. PMID: 23534542.
12. Choi PS, Zakhary L, Choi WY, Caron S, Alvarez-Saavedra E, Miska EA, McManus M, Harfe B, Giraldez AJ, Horvitz HR, Schier AF, Dulac C. Members of the miRNA-200 family regulate olfactory neurogenesis. Neuron. 2008 Jan 10;57(1):41-55. doi: 10.1016/j.neuron.2007.11.018. PMID: 18184563; PMCID: PMC2204047
13. Beclin C, Follert P, Stappers E, Barral S, Coré N, Chevigny A, Magnone V, Lebrigand K, Bissels U, Huylebroeck D, Bosio A, Barbry P, Seuntjens E, Cremer H. Corrigendum: miR-200 family controls late steps of postnatal forebrain neurogenesis via Zeb2 inhibition. Sci Rep. 2016 Dec 21;6:39368. doi: 10.1038/srep39368. Erratum for: Sci Rep. 2016 Oct 21;6:35729. doi: 10.1038/srep35729. PMID: 28000724; PMCID: PMC5175142.
14. Zhang J, Gao Y, Yu M, Wu H, Ai Z, Wu Y, Liu H, Du J, Guo Z, Zhang Y. Retinoic Acid Induces Embryonic Stem Cell Differentiation by Altering Both Encoding RNA and microRNA Expression. PLoS One. 2015 Jul 10;10(7):e0132566. doi: 10.1371/journal.pone.0132566. PMID: 26162091; PMCID: PMC4498831.
15. Tseng JH, Bisogna M, Hoang LN, Olvera N, Rodriguez-Aguayo C, Lopez-Berestein G, Sood AK, Levine DA, Jelinic P. miR-200c-driven Mesenchymal-To-Epithelial Transition is a Therapeutic Target in Uterine Carcinosarcomas. Sci Rep. 2017 Jun 15;7(1):3614. doi: 10.1038/s41598-017-03972-7. PMID: 28620240; PMCID: PMC5472620.
16. Chen D, Zhang Y, Wang J, Chen J, Yang C, Cai K, Wang X, Shi F, Dou J. MicroRNA-200c overexpression inhibits tumorigenicity and metastasis of CD117+CD44+ ovarian cancer stem cells by regulating epithelial-mesenchymal transition. J Ovarian Res. 2013 Jul 10;6(1):50. doi: 10.1186/1757-2215-6-50. PMID: 23842108; PMCID: PMC3729499.
17. Jin T, Suk Kim H, Ki Choi S, Hye Hwang E, Woo J, Suk Ryu H, Kim K, Moon A, Kyung Moon W. microRNA-200c/141 upregulates SerpinB2 to promote breast cancer cell metastasis and reduce patient survival. Oncotarget. 2017 May

16;8(20):32769-32782. doi: 10.18632/oncotarget.15680. PMID: 28427146; PMCID: PMC5464826.

18. Yadav SK, Dhuri K, Gamiotea-Turro D, Cormier MK, Patel V, Yadawa AK, Pathuri M, Bahal R, Verma R. Exploring the therapeutic potential of syPNA-141: Pharmacodynamics and mechanistic insights during ischemic stroke recovery. Mol Ther Nucleic Acids. 2024 Oct 9;35(4):102355. doi: 10.1016/j.omtn.2024.102355. PMID: 39507400; PMCID: PMC11539414.
19. Wu Q, Ye X, Xiong Y, Zhu H, Miao J, Zhang W, Wan J. The Protective Role of microRNA-200c in Alzheimer's Disease Pathologies Is Induced by Beta Amyloid-Triggered Endoplasmic Reticulum Stress. Front Mol Neurosci. 2016 Dec 8;9:140. doi: 10.3389/fnmol.2016.00140. PMID: 28008308; PMCID: PMC5143617.
20. Liu B, Du R, Zhou L, Xu J, Chen S, Chen J, Yang X, Liu DX, Shao ZM, Zhang L, Yu Z, Xie N, Guan JL, Liu S. miR-200c/141 Regulates Breast Cancer Stem Cell Heterogeneity via Targeting HIPK1/β-Catenin Axis. Theranostics. 2018 Nov 10;8(21):5801-5813. doi: 10.7150/thno.29380. PMID: 30613263; PMCID: PMC6299432.
21. Ji ML, Jiang H, Zhang XJ, Shi PL, Li C, Wu H, Wu XT, Wang YT, Wang C, Lu J. Preclinical development of a microRNA-based therapy for intervertebral disc degeneration. Nat Commun. 2018 Nov 28;9(1):5051. doi: 10.1038/s41467-018-07360-1. PMID: 30487517; PMCID: PMC6262020.
22. Hoefert JE, Bjerke GA, Wang D, Yi R. The microRNA-200 family coordinately regulates cell adhesion and proliferation in hair morphogenesis. J Cell Biol. 2018 Jun 4;217(6):2185-2204. doi: 10.1083/jcb.201708173. Epub 2018 Mar 30. PMID: 29602800; PMCID: PMC5987720.
23. Guan T, Dominguez CX, Amezquita RA, Laidlaw BJ, Cheng J, Henao-Mejia J, Williams A, Flavell RA, Lu J, Kaech SM. ZEB1, ZEB2, and the miR-200 family form a counterregulatory network to regulate $CD8^+$ T cell fates. J Exp Med. 2018 Apr 2;215(4):1153-1168. doi: 10.1084/jem.20171352. Epub 2018 Feb 15. PMID: 29449309; PMCID: PMC5881466.
24. Wu MJ, Chen YS, Kim MR, Chang CC, Gampala S, Zhang Y, Wang Y, Chang CY, Yang JY, Chang CJ. Epithelial-Mesenchymal Transition Directs Stem Cell Polarity via Regulation of Mitofusin. Cell Metab. 2019 Apr 2;29(4):993-1002.e6. doi: 10.1016/j.cmet.2018.11.004. Epub 2018 Dec 6. PMID: 30527740.

25. Xu L, Griffiths B, Sun X, Greer M, Chang H, McMillin E, Manis E, Russo I, Dean CAJ, Stary CM. Conditional neuronal deletion of microRNA-141/200c cluster, but not microRNA-181a/b-1 cluster, is protective against experimental stroke in male mice. Physiol Rep. 2025 Aug;13(15):e70505. doi: 10.14814/phy2.70505. PMID: 40810631; PMCID: PMC12351801.
26. Tran M, Lee SM, Shin DJ, Wang L. Loss of miR-141/200c ameliorates hepatic steatosis and inflammation by reprogramming multiple signaling pathways in NASH. JCI Insight. 2017 Nov 2;2(21):e96094. doi: 10.1172/jci.insight.96094. PMID: 29093267; PMCID: PMC5752284.
27. Mostofa MG, Tran M, Gilling S, Lee G, Fraher O, Jin L, Kang H, Park YK, Lee JY, Wang L, Shin DJ. MicroRNA-200c coordinates HNF1 homeobox B and apolipoprotein O functions to modulate lipid homeostasis in alcoholic fatty liver disease. J Biol Chem. 2022 Jun;298(6):101966. doi: 10.1016/j.jbc.2022.101966. Epub 2022 Apr 20. PMID: 35460694; PMCID: PMC9127369.
28. Tran M, Gilling S, Wu J, Wang L, Shin DJ. miR-141/200c contributes to ethanol-mediated hepatic glycogen metabolism. Mol Metab. 2024 Jun;84:101942. doi: 10.1016/j.molmet.2024.101942. Epub 2024 Apr 18. PMID: 38642890; PMCID: PMC11060962.
29. Raja, R., Dumontier, E., Phen, A., & Cloutier, J. F. (2024). Insertion of a neomycin selection cassette in the Amigo1 locus alters gene expression in the olfactory epithelium leading to region-specific defects in olfactory receptor neuron development. *Genesis*, 62, e23594.
30. Testa G, Schaft J, van der Hoeven F, Glaser S, Anastassiadis K, Zhang Y, Hermann T, Stremmel W, Stewart AF. A reliable lacZ expression reporter cassette for multipurpose, knockout-first alleles. Genesis. 2004 Mar;38(3):151-8. doi: 10.1002/gene.20012. PMID: 15048813.
31. Pham CT, MacIvor DM, Hug BA, Heusel JW, Ley TJ. Long-range disruption of gene expression by a selectable marker cassette. Proc Natl Acad Sci U S A. 1996 Nov 12;93(23):13090-5. doi: 10.1073/pnas.93.23.13090. PMID: 8917549; PMCID: PMC24051.
32. Wu Y, Wang C, Sun H, LeRoith D, Yakar S. High-efficient FLPo deleter mice in C57BL/6J background. PLoS One. 2009 Nov 26;4(11):e8054. doi: 10.1371/journal.pone.0008054. PMID: 19956655; PMCID: PMC2777316.

33. Kranz A, Fu J, Duerschke K, Weidlich S, Naumann R, Stewart AF, Anastassiadis K. An improved Flp deleter mouse in C57Bl/6 based on Flpo recombinase. Genesis. 2010 Aug;48(8):512-20. doi: 10.1002/dvg.20641. PMID: 20506501.
34. Raymond CS, Soriano P. High-efficiency FLP and PhiC31 site-specific recombination in mammalian cells. PLoS One. 2007 Jan 17;2(1):e162. doi: 10.1371/journal.pone.0000162. PMID: 17225864; PMCID: PMC1764711.
35. Rishik S, Hirsch P, Grandke F, Fehlmann T, Keller A. miRNATissueAtlas 2025: an update to the uniformly processed and annotated human and mouse non-coding RNA tissue atlas. Nucleic Acids Res. 2025 Jan 6;53(D1):D129-D137. doi: 10.1093/nar/gkae1036. PMID: 39540421; PMCID: PMC11701691.
36. Branda CS, Dymecki SM. Talking about a revolution: The impact of site-specific recombinases on genetic analyses in mice. Dev Cell. 2004 Jan;6(1):7-28. doi: 10.1016/s1534-5807(03)00399-x. PMID: 14723844.
37. 27. McBurney MW, Mai T, Yang X, Jardine K. Evidence for repeat-induced gene silencing in cultured Mammalian cells: inactivation of tandem repeats of transfected genes. Exp Cell Res. 2002 Mar 10;274(1):1-8. doi: 10.1006/excr.2001.5443. PMID: 11855851.
38. Skarnes WC, Auerbach BA, Joyner AL. A gene trap approach in mouse embryonic stem cells: the lacZ reported is activated by splicing, reflects endogenous gene expression, and is mutagenic in mice. Genes Dev. 1992 Jun;6(6):903-18. doi: 10.1101/gad.6.6.903. PMID: 1592261.
39. Nair P, Steel KP, Lewis MA. Investigating the effects of a cryptic splice site in the En2 splice acceptor sequence used in the IKMC knockout-first alleles. Mamm Genome. 2024 Dec;35(4):633-644. doi: 10.1007/s00335-024-10071-2. Epub 2024 Oct 1. PMID: 39354111; PMCID: PMC11522132.
40. Stanford WL, Caruana G, Vallis KA, Inamdar M, Hidaka M, Bautch VL, Bernstein A. Expression trapping: identification of novel genes expressed in hematopoietic and endothelial lineages by gene trapping in ES cells. Blood. 1998 Dec 15;92(12):4622-31. PMID: 9845528.
41. He Y, Nan D, Wang H. Role of Non-Receptor-Type Tyrosine Phosphatases in Brain-Related Diseases. Mol Neurobiol. 2023 Nov;60(11):6530-6541. doi: 10.1007/s12035-023-03487-5. Epub 2023 Jul 17. PMID: 37458988.

42. Xu T, Fan X, Tan Y, Yue Y, Chen W, Gu X. Expression of PHB2 in rat brain cortex following traumatic brain injury. Int J Mol Sci. 2014 Feb 21;15(2):3299-318. doi: 10.3390/ijms15023299. PMID: 24566151; PMCID: PMC3958913.
43. Whitton C, Palmer E, Alkuraya F. *ATN1*-Related Neurodevelopmental Disorder. 2022 Aug 25. In: Adam MP, Feldman J, Mirzaa GM, Pagon RA, Wallace SE, Amemiya A, editors. GeneReviews® [Internet]. Seattle (WA): University of Washington, Seattle; 1993–2025. PMID: 36007104.
44.